M. W. Brown, K. J. Miller,* U. S. Fernando,* J. R. Yates*, and D. K. Suker*

Aspects of Multiaxial Fatigue Crack Propagation

REFERENCE Brown, M. W., Miller, K. J., Fernanado, U. S., Yates, J. R. and Suker, D. K., **Aspects of multiaxial fatigue crack propagation**, *Multiaxial and Fatigue Design*, ESIS 21 (Edited by A. Pineau, G. Cailletaud, and T. C. Lindley) 1996, Mechanical Engineering Publications, London, pp. 317–334.

ABSTRACT Fatigue under multiaxial loading is a failure process which is best understood by examining crack propagation mechanics, since it is the physical growth of cracks that controls the accumulation of damage. Cracks form and grow initially in a shear Stage I mode under the dominant influence of local microstructure. Once Stage I is complete, three further modes of growth are known which may be selected by the material to produce the final failure, namely (a) opening mode growth of Stage II, (b) shear mode tearing under Mode III high strain loading, and (c) mixed mode propagation on a shear plane with a nonproportional shear plus opening mode load history. A life prediction methodology is outlined and an example is discussed for a medium carbon steel loaded in torsion.

1 Introduction

Fatigue failure is a problem associated with generation and growth of cracks. If a proper physical understanding of the mechanisms involved is to be gained, engineering failures should be interpreted in terms of crack growth phenomena. Whereas an empirical approach to multiaxial fatigue is often pursued in view of the complexity of the crack propagation problem, lasting solutions for failure prevention will only be achieved by addressing the mechanics of fracture. Three basic modes of crack loading are identified in fracture mechanics, namely (a) Mode II shear loading, which relates to Stage I fatigue crack extension, (b) Mode I tensile or opening loading, which relates to Stage II fatigue crack extension, and (c) Mode III antiplane shear loading, which relates to Stage III fatigue cracks. Each mode of growth can be observed in practice. Shear mode cracks with three-dimensional shapes involve mixed mode states, ranging from pure Mode II to pure Mode III around their boundaries. Often with superimposed Mode I, they are found with torsion in shafts, turbogenerators, nonproportional low cycle fatigue (LCF), rolling contact, fretting, and Al-Li alloys, for examples.

*Sirius, The University of Sheffield, Mappin Street, Sheffield, S1 3JD, UK.

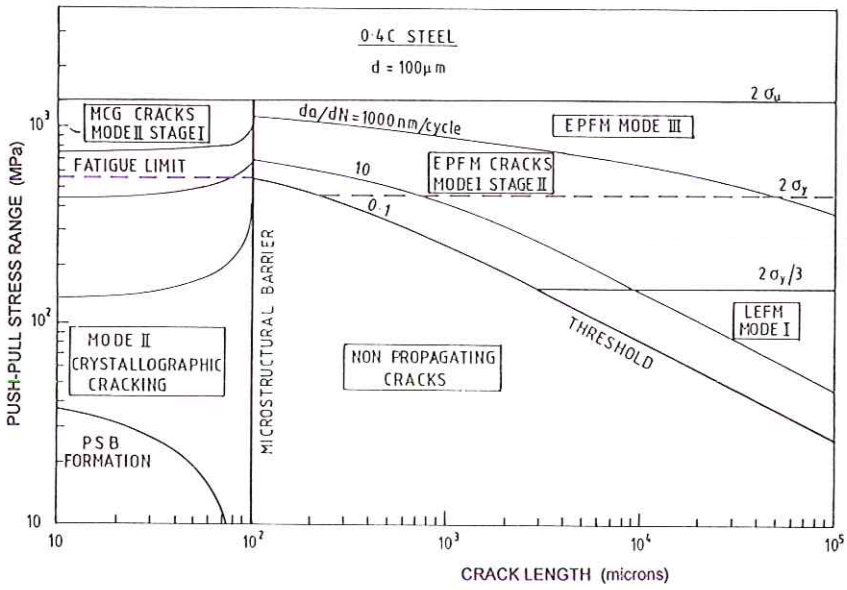

Fig 1 Fatigue crack growth map for medium carbon steel under uniaxial loading, showing regimes of Stage I microstructural crack growth (MCG), Stage II opening mode threshold and growth (LEFM and EPFM), Mode III shear, with contours of constant propagation rate.

One of the most important aspects of multiaxial fatigue crack growth (FCG) is the speed of a crack, which determines the endurance of a component. However various other pertinent questions arise, concerning choice between linear elastic fracture mechanics (LEFM) and elastoplastic fracture mechanics (EPFM), the limits of validity for corresponding FCG rules, the preferred mode of propagation, and the criteria for transfer from one mode to another. There are multiaxial aspects to each question, for which some answers can be found by reference to a 'fatigue diagram'.

For uniaxial loading a 'fatigue diagram' has been developed (**1**), showing which growth mode is preferred as a function of both crack length and applied stress range. The diagram has been derived for fully reversed cycling, with crack length being small compared to component size. A fatigue diagram for a 0.4C steel is shown in Fig. 1, assuming a prior austenite grain size (or microstructural dimension) of 100 μm (**2**). In this case shear cracking is observed for any crack length less than the dominant microstructural dimension d. Using FCG laws and the stable cyclic stress–strain curve, contours of constant FCG rate have been found for 0.1, 10 and 1000 nm/cycle. The Mode II regime is bounded by

(a) a vertical line at the microstructural barrier;
(b) a lower bound for Persistent Slip Band formation (there can be no propagation without cyclic plasticity in a surface grain);

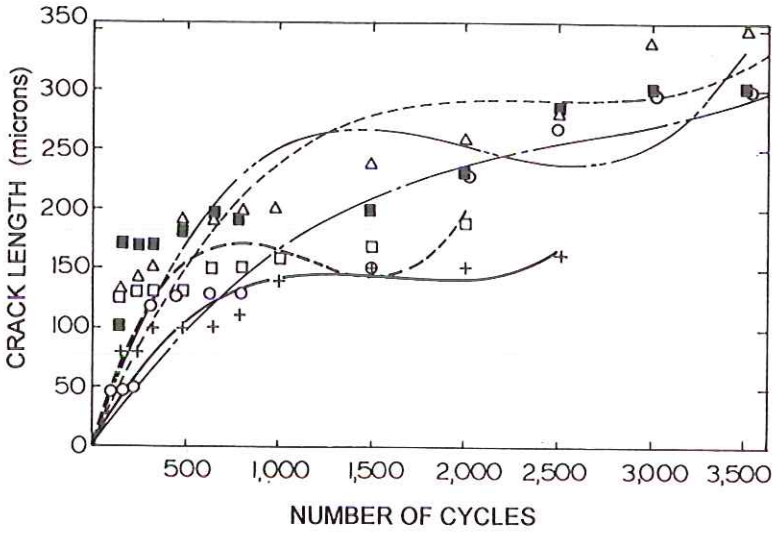

Fig 2 Relationship between measured crack length and number of cycles applied, for five short cracks in torsional low-cycle fatigue of medium carbon steel (3% shear strain range, 491 MPa stress range, endurance of 4090 cycles). Lines are fitted cubic polynomials to highlight immediate crack initiation, then retardation after passing through the microstructural barrier.

(c) an upper bound of twice tensile strength (σ_u) for fully reversed loading.

Above the fatigue limit, Mode I crack propagation becomes possible if not only the Mode I threshold is exceeded, but also the growth mechanism is easier (or faster) than Mode II crystallographic extension. Thus fast Stage I growth precedes a relatively dormant region of Mode I close to threshold (3) – see Fig. 2. Between the microstructural barrier and the Mode I threshold line, there is a region of nonpropagating cracks, where no growth is possible. This region is bounded at the highest point by the material fatigue limit. Mode III cracking is found only at high stress ranges. The Mode I LEFM regime is clearly defined between the threshold line and the upper limit of two thirds of the cyclic yield stress, ensuring small-scale yielding. Although Fig. 1 has been drawn for uniaxial loading, a similar diagram can be drawn for any multiaxial stress state, using the FCG equations for Modes I, II and III.

2 Stages of Crack Behaviour

All materials deform, elastically and plastically, to various degrees and will continue to do so as the applied loading in a fatigue cycle accumulates until one or more fracture processes occur. The extent of elastic and plastic deformation prior to fracture is dependent on the material under study, the test temperature, the environment and the applied load. Although elastic behaviour

is relatively well understood, plasticity and the transition between elastic and plastic behaviour, certainly for out-of-phase situations, is not; and current knowledge is largely based on experimental findings. This is particularly true for three-dimensional studies. Consequently, theories of three-dimensional deformation behaviour still dominantly depend on empirical hypotheses such as von Mises equivalent strain, Tresca yield criterion and Neuber relationships.

Current knowledge pertaining to three-dimensional fracture problems is much more limited since, as well as material, temperature, stress and environmental variables, there are the problems relating to defects; namely their size, shape, position and orientation, particularly in respect to the geometry of the specimen, component or structure, together with the geometry of the external loading system with respect to the defect under consideration. Leblond (**4**) has recently solved the problem of a three-dimensional crack in an infinite elastically stressed body, but the solution of a three-dimensional defect (crack, void, notch) in an elastoplastic body will remain unsolved for many years.

In fatigue fracture studies, however, some simplifications are possible which assist the engineer to reach physically understandable and acceptable solutions.

(1) One may assume that all engineering materials, components and structures have defects, ranging from one or two microns up to, say, a metre in length. The best possible prepared surface of a polycrystalline metal specimen can be presumed after plastic flow to have a defect of the order of one tenth of a micron in depth. Because of this, studies indicate that 'initiation' can be ignored (as shown in Fig. 2) and the problem of whether or not a defect will propagate simplified.

(2) Many fatigue cracks extend by just two processes, as in Stage I crack growth which is dominated by shear stresses, and a Stage II crack growth process which is dominated by tensile stresses (**5, 6**), see Fig. 3. In this respect, the two-stage classification of cracking is more practical than the more often used three-mechanism LEFM approach of Modes I, II and III, which considers the external mechanical loading system rather than the physical processes which must be accommodated by the material in which a crack is advancing.

It follows that the generalized three-dimensional fatigue fracture theory (**7**) is a reasonable start to understanding multiaxial fatigue behaviour since essentially the theory is based on the physical processes involved in crack extension. Analysis considers the stresses and strains that occur on the possible planes of Stage I and Stage II cracks, and then follows the Pineau theory (**8**) in which the dominant process will be that which produces the fastest FCG rate. Using this reasoning, three important considerations need to be noted. First, fatigue failure can occur which would not otherwise be predicted by any of the classical deformation-based theories. For example, when the three-dimensional stresses are maintained constant in magnitude but rotate, planes of Stage I and Stage II crack growth will witness a cyclically variable stress–strain state. Secondly

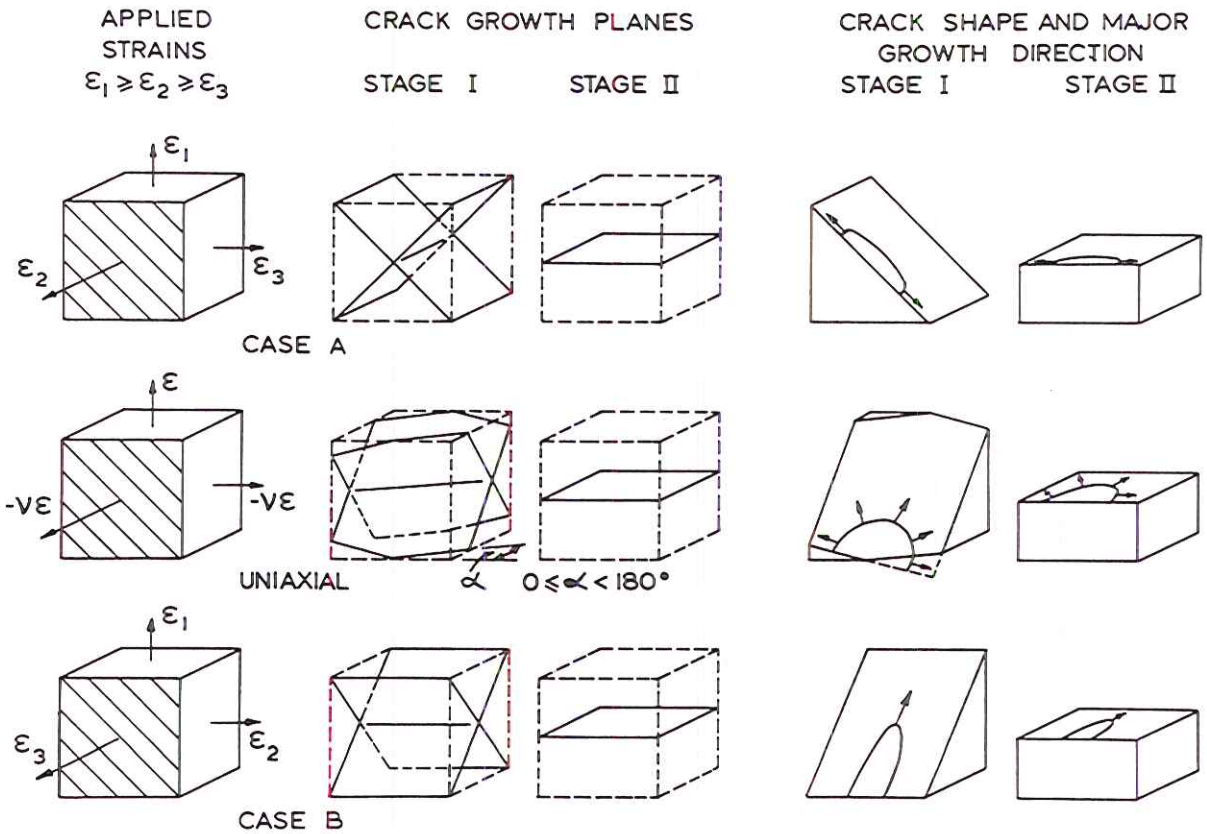

Fig 3 Crack growth planes and shapes for shear mode and opening mode in multiaxial fatigue. (Case A typical of torsion shear loads, Case B typical of plane strain notches and thermal loads).

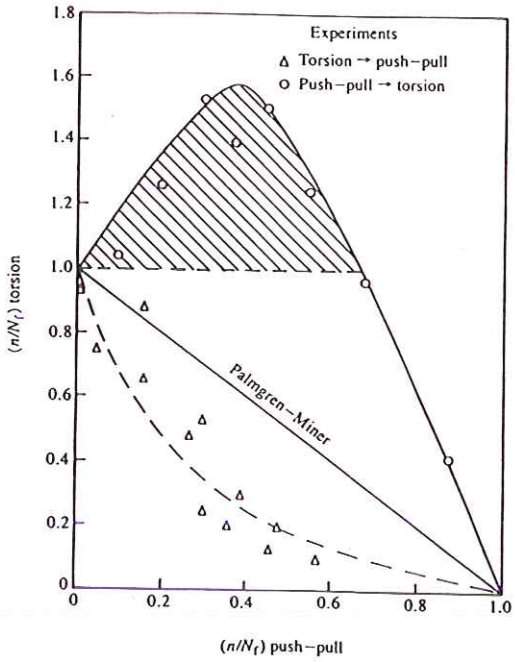

Fig 4 Effect of sequential loading, dependent on which cracking system is applied initially – note that Palmgren–Miner hypothesis is approximately applicable if a single cracking system is dominant throughout lifetime.

the geometry of a specimen plays an important role, particularly in terms of changing constraints on a crack as it grows. Indeed, it is possible to show that one three-dimensional theory of fatigue is better than another theory simply by choosing a geometry that assists changes in the crack growth process. Thirdly it is vitally important to separate out the material response to a three-dimensional loading system from geometry effects.

To illustrate this final point, Fig. 4 shows an example of how, for stress–strain states which give the same endurance in reversed torsion and push-pull loading ($R = -1$), the fatigue lifetime can be dramatically reduced if the stress–state is initially applied in torsion and then in push-pull. Alternatively an unusual increase in lifetime can be gained if push-pull is applied before application of the torsion loading. The reduction in lifetime is primarily due to a broad Stage I torsional crack naturally continuing propagation in Stage II. However Stage I cracks generated in push-pull hinder the development and extension of shear cracks in torsion, because they form on 45° planes unfavourable for subsequent FCG.

2.1 *The Stage I short crack growth equation*

Hobson (**2**) proposed an equation which described the development of fatigue

cracks within the first grain of a polycrystalline material under uniaxial LCF with strain range $\Delta\varepsilon$, accounting for the microstructural influences on crack growth rate (in his case, grain boundary triple points) in terms of a barrier for propagation, d, such that

$$da/dN = A(\Delta\varepsilon)^m(d - a) \tag{1}$$

where d is the microstructural length parameter, A and m are material constants and a is the surface crack length. This equation embodies the remaining plastic slip band $(d - a)$ between the crack tip and the barrier, a parameter which has also been predicted in dislocation models of the mechanism of Stage I cracking. Equation (1) may be extended to torsion, where crack depth c is used instead of surface length a, with the aspect ratio $\beta = 2c/a$. For shear mode cracks of less than one grain size, the Mode II propagation rate is

$$[dc/dN]_{II} = 36700(\Delta\gamma)^{3.51}(\beta d/2 - c) \tag{2}$$

where $\beta d/2 = 116\ \mu m$ for the carbon steel used by Hobson. The units selected for c and d must be mutually consistent in the equation, and the strain is the engineering shear strain. Fatigue life can be determined by integrating equation (2) from $c = 0$ up to the transitional crack length c_i, to give

$$N_{II} = 0.0000273(\Delta\gamma)^{-3.51} \ln(\beta d/(\beta d - 2c_i)) \tag{3}$$

where N_{II} is the number of cycles required to initiate and grow a Stage I Mode II crack.

2.2 *Opening mode crack growth equation*

Mode I crack growth may be described for linear elastic conditions by a Paris-type law (6)

$$da/dN = C[(\Delta K)^m - (\Delta K_{th})^m] \tag{4}$$

where ΔK and ΔK_{th} are range of stress intensity factor and the threshold value respectively. The terms C and m are material constants, whose values can frequently be found from the literature. It is proposed here that a strain intensity factor $(\Delta K/E)$ controls both LEFM and EPFM fatigue crack growth (6), giving a general expression for push-pull as follows.

$$da/dN = C(\Delta\varepsilon)^m a - D \tag{5}$$

where D represents the threshold. Equations (4) and (5) are equivalent when $m = 2$.

Using the crack depth c instead of surface length a, and replacing $\Delta\varepsilon$ with an equivalent strain range (5) derived from the strain intensity factor $(\Delta K/E)$, this equation was fitted to Hobson's push-pull data, with the aspect ratio β assumed equal to 1, to give

$$[dc/dN]_I = 0.427(\Delta\gamma)^{2.06}c - 0.00212 \tag{6}$$

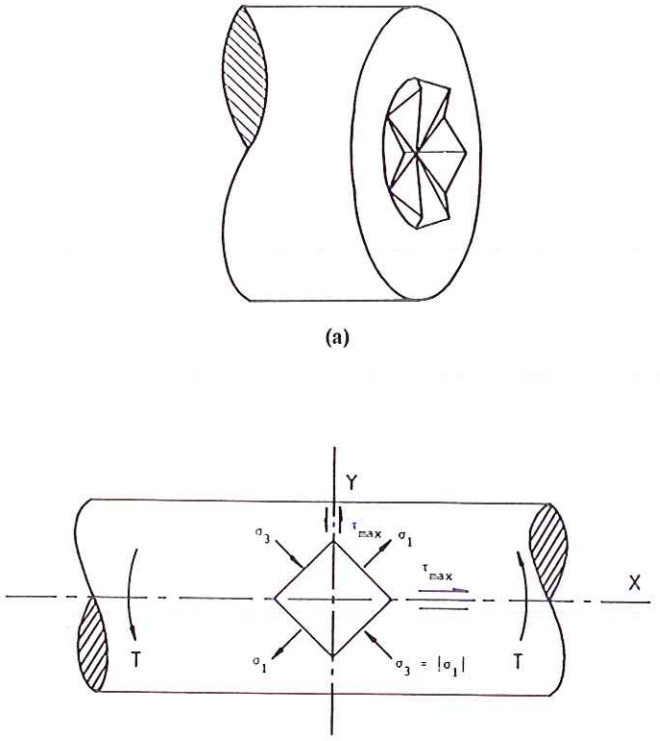

(a)

(b)

Fig 5 Development of shear mode torsional cracks: (a) Mode I facets formed in a Mode III fatigue specimen; (b) state of stress in torsion.

where dc/dN is in μm/cycle and c is in μm. Equation (6) gives the propagation rate of a Mode I crack under torsional loading. Integrating this equation from c_i (crack depth for Stage I to Stage II transition) to c_d (final crack depth for Mode I), gives the Mode I propagation life.

$$N_I = 2.35(\Delta\gamma)^{-2.06} \ln[(c_d - 0.0050(\Delta\gamma)^{-2.06})/(c_i - 0.0050(\Delta\gamma)^{-2.06}] \quad (7)$$

N_I is the endurance where the crack grows on a plane normal to the maximum principal strain.

3 Mode III Crack Propagation

Mode III fatigue threshold and FCG tests are invariably conducted on circumferentially notched or slit cylindrical specimens loaded in torsion, giving two characteristic fracture surfaces. Under elastic loading, at low stress intensity factor ranges, a surface made up from inclined facets occurs, and is often termed

a 'factory roof' fracture surface. These are formed by a number of intersecting Mode I cracks, see Fig. 5a. Under fully reversed loading, two sets of 45° facets are produced in response to the two maximum principal stress directions. Tests by Hourlier *et al.* (**8**) demonstrated that only one set of facets is formed in tests at a load ratio $R = 0$ and the interlinking ligaments failed by a ductile fracture mechanism. Similar fracture facets have been observed by Sommer (**9**) in glass broken under a static torsion load.

The other fracture morphology seen in torsion tests comprises a flat, smeared surface in which extensive rubbing has occurred. Ritchie *et al.* (**10**) noted that such specimens became hot during testing, exuding material from the crack. It has been suggested that flat surfaces are formed by the abrasion of the 'factory roof' surface (**8, 11**), but other observations of a transition from small 'factory roof' facets to flat fracture (**12**) would indicate that the flat surface is formed by a true Mode III mechanism operating on the planes of maximum shear strain, see Fig. 5b.

A transition from flat to faceted FCG is commonly observed, and is often associated with

(a) long fatigue crack lengths (**8, 13**) as the increasing dissipation of torque on the crack faces decreases the strength of the crack tip stress field,
(b) large specimen diameters which allow the crack tip plasticity to be localized (**14,15**),
(c) high strength materials (**10**).

The conclusion drawn is that true Mode III FCG is associated with plastic shear and conditions which favour extensive plasticity, such as low yield stress, small specimens and high torques.

3.1 *Threshold conditions*

The two-crack growth mechanisms for Mode III lead to two possible threhold conditions. Pook *et al.* (**16,17**) regarded the ease of formation and growth of Mode I branch cracks as the important condition for determining torsional fatigue failure. Tschegg (**18**) considered the true Mode III threshold to be the lowest stress intensity factor range at which Mode III flat crack growth occurred. Further threshold conditions for the onset of microscopic shear mode crack growth can also be considered (**12**). A component in service may survive indefinitely if the stress intensity factor range is below that required for the propagation of Mode I branch (facet) cracks, since Mode III crack growth is associated with high strains and short fatigue lives.

Prediction of the branch crack threshold condition under Mode III loading has been investigated (**16**) through analysis of the main crack tip stress field and by considering the crack opening displacement in the direction of the branch cracks. Yates and Miller (**19**) suggested that the Mode I branch crack threshold under Mode III loading was about $\Delta K_{\mathrm{IIIth}} = 0.8\Delta K_{\mathrm{Ith}}$ whereas Pook (**20**)

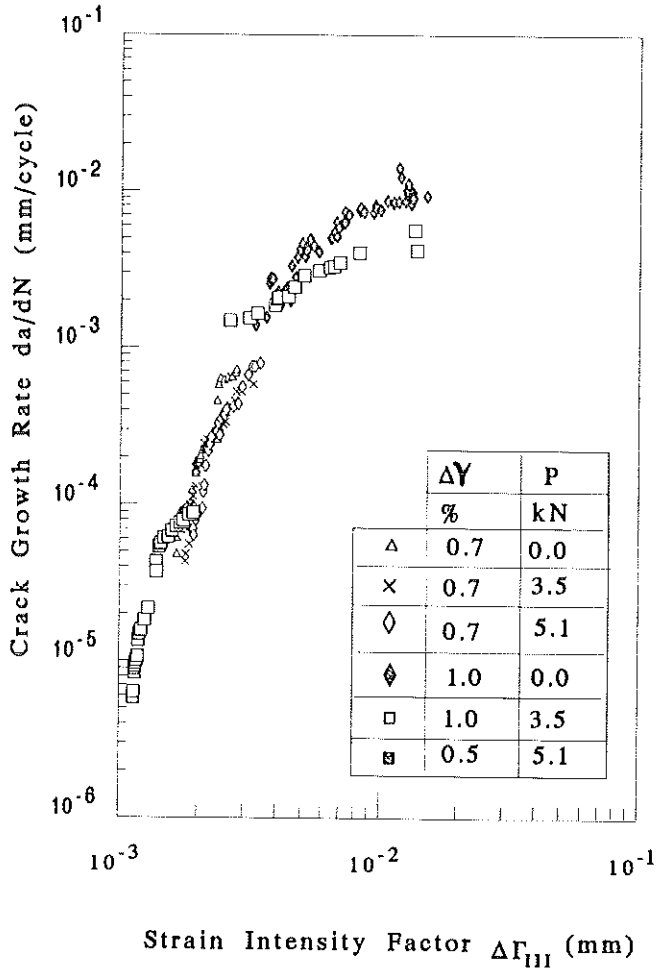

Fig 6 Mode III crack growth rate for medium carbon steel, versus strain intensity factor. Circumferentially cracked specimens were loaded with a torsional strain range $\Delta\gamma$ and a static end load P.

suggested that it lay in the region $\Delta K_{\mathrm{IIIth}} = 1.0\Delta K_{\mathrm{Ith}}$ to $1.35\Delta K_{\mathrm{Ith}}$. This is an area that warrants further investigation.

3.2 *Mode III fatigue crack propagation rates*

The development of general fatigue lifetime methodologies for industry requires the determination of expressions for crack propagation rates under all modes of crack extension. Some success has been achieved by relating Mode III crack growth rates to the extent of the Mode III plastic zone r_y, via the related parameter, Γ_{III}, the strain intensity factor (Fig. 6)

$$\Gamma_{III} = \gamma_y r_y \tag{8}$$

which in the limit of small-scale yielding reduces to half the Mode III crack sliding displacement. Here γ_y is the shear strain at yield. Hay and Brown (**12**) suggested that, for a and Γ_{III} in μm

$$da/dN = 0.1\Delta\Gamma_{III}^2 \tag{9}$$

was a reasonable upper bound to the Mode III growth rates observed in low alloy steels. Mode III plastic zone sizes, and hence $\Delta\Gamma_{III}$, can be determined using the methods outlined by McClintock and Tschegg (**21**) or Yates (**15**). Prediction of Mode III FCG rates is made more complicated than in Mode I because of the crack flank friction discussed earlier, which produces decreasing FCG rates with increasing crack length at constant $\Delta\Gamma_{III}$. In Fig. 6, this problem was avoided by using (a) effective $\Delta\Gamma_{III}$, and (b) a tensile end load to hold fracture faces apart.

3.3 *Mean stress effects in Mode III*

Little work has been conducted on the importance of mean stress on Mode III FCG and threshold behaviour. Hurd and Irving (**22**) demonstrated that Mode III cracks in torsion specimens had a tendency to branch more readily at $R = 0.08$ than at $R = -1$. Threshold studies (**23**, **24**) on circumferentially slit specimens tested in pure torsion indicated that the onset of Mode I facet growth was independent of stress ratio. This is not surprising as the usual mechanisms of roughness and oxide induced closure, which play an important part in Mode I thresholds, cannot operate in slit specimens.

The considerable technical difficulties in pre-cracking round specimens to perform pure Mode III tests have tended to discourage workers in this area. Furthermore, the studies on Mode I + II thresholds (**25**) suggest that the method of pre-cracking can influence the subsequent mixed mode crack propagation behaviour. This problem deserves attention in the future. Mode II thresholds have received more interest, being reported in a recent conference (**26**). Mode II extension is difficult to achieve, except for (a) short Stage I cracks, (b) nonpropagating cracks below the branching threshold, and (c) nonproportional loading.

3.4 *Mode III shear crack growth equation*

When analysing the FCG problem in shear mode with high plasticity, LEFM cannot supply a sound basis on which to characterize crack growth rate. A general EPFM Mode III equation, fitted to data generated on circumferentially cracked specimens of medium carbon steel tested at room temperature (Fig. 6), is (in μm/cycle)

$$[dc/dN]_{III} = 0.03(\Delta\Gamma_{III})^{2.9} - 0.04 \tag{10}$$

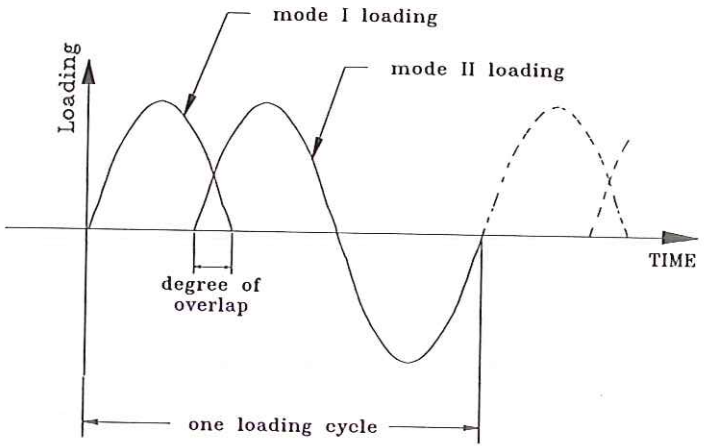

Fig 7 Mixed Mode I/II sequential loading, showing overlap between opening and shear cycles.

where $\Delta\Gamma_{III}$ and c are given in μm. The strain intensity factor is defined in torsionally stressed bars as (**15**)

$$\Gamma_{III} = \gamma_y c[(\sec(\pi T_A/2T_L))^{Y^2} - 1] \tag{11}$$

and represents the level of strain imposed around the crack tip. Here T_A and T_L are the applied and limit load values of torque, and Y is the geometry factor for the Mode III elastic stress intensity factor for the cracked bar. Equation (10) is integrated numerically from c_d to c_f (which are the final Mode I and failure crack depths respectively) to estimate the fatigue life of a specimen N_{III} obtained under high strain loading for Mode III cracking on a shear plane.

4 Nonproportional Loading

To date there has only been limited study of nonproportional loading effects for FCG. It is generally known that for out-of-phase strain controlled LCF, tension–torsion specimens exhibit reduced lifetimes (**5**), which implies that propagation rates are faster with nonproportional straining. The cracks experience a mixed mode cycle, as opening and shear stress intensities vary out-of-phase. A crack cannot be classified as either opening or shear mode, but cracks extend on planes experiencing the maximum range of shear strain.

A similar effect is observed in mixed mode sequential loading of rail steel. Figure 7 shows a loading history typical of that experienced in rolling contact fatigue under wet conditions, where FCG is observed on planes experiencing high shear (**27**). FCG tests on cruciform specimens with 45° starter cracks permit simulation of this sequential loading history. Collected results for rail steel are

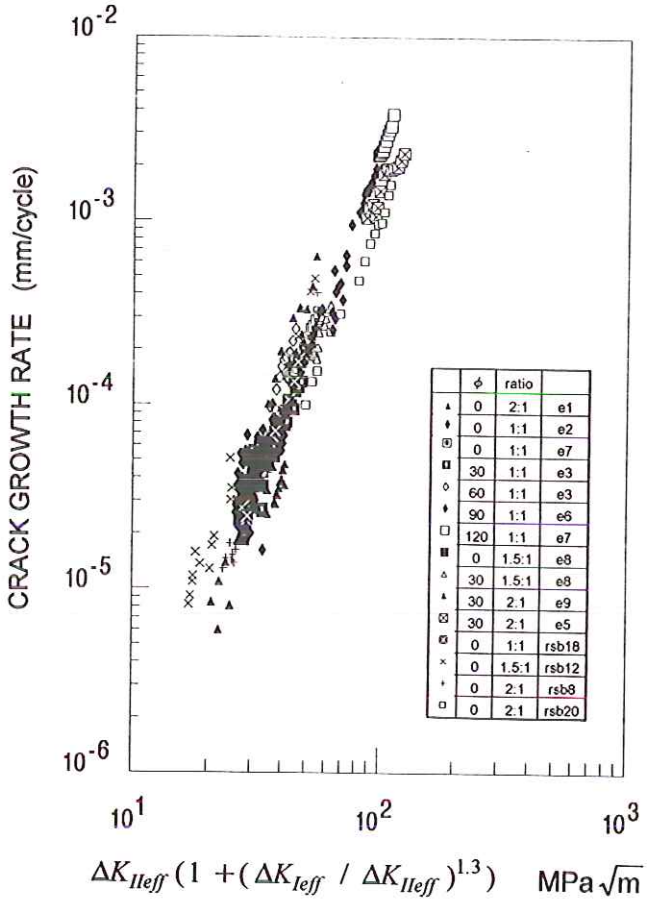

Fig 8 Collation of co-planar crack growth on the maximum shear plane in rail steel, versus modified effective Mode II stress intensity range. Key shows overlap ϕ of stress intensity waveforms for Mode I and II cycles in degrees (Fig. 7), and the ratio ΔK_{II}: ΔK_{I}. Experiment numbers where appropriate identify source of data – e1 to e9 (28) and rsb8 to rsb20 (27).

shown in Fig. 8, for propagation on the plane of maximum shear (**28**), where effective ΔK values are used to allow for the influence of crack face friction. The shear-dominated interactive mixed mode FCG rate for this mechanism is given by

$$[dc/dN]_{II/I} = 0.000614[\Delta K_{IIeff}(1 + (\Delta K_{Ieff}/\Delta K_{IIeff})^{1.3})]^{3.21} \text{ nm/cycle} \quad (12)$$

If the effective Mode I stress intensity drops below a critical level, the cracks branch, reverting to a Mode I plane. Nevertheless this shear mode mechanism is faster than the Mode I response, even for the LEFM conditions employed here.

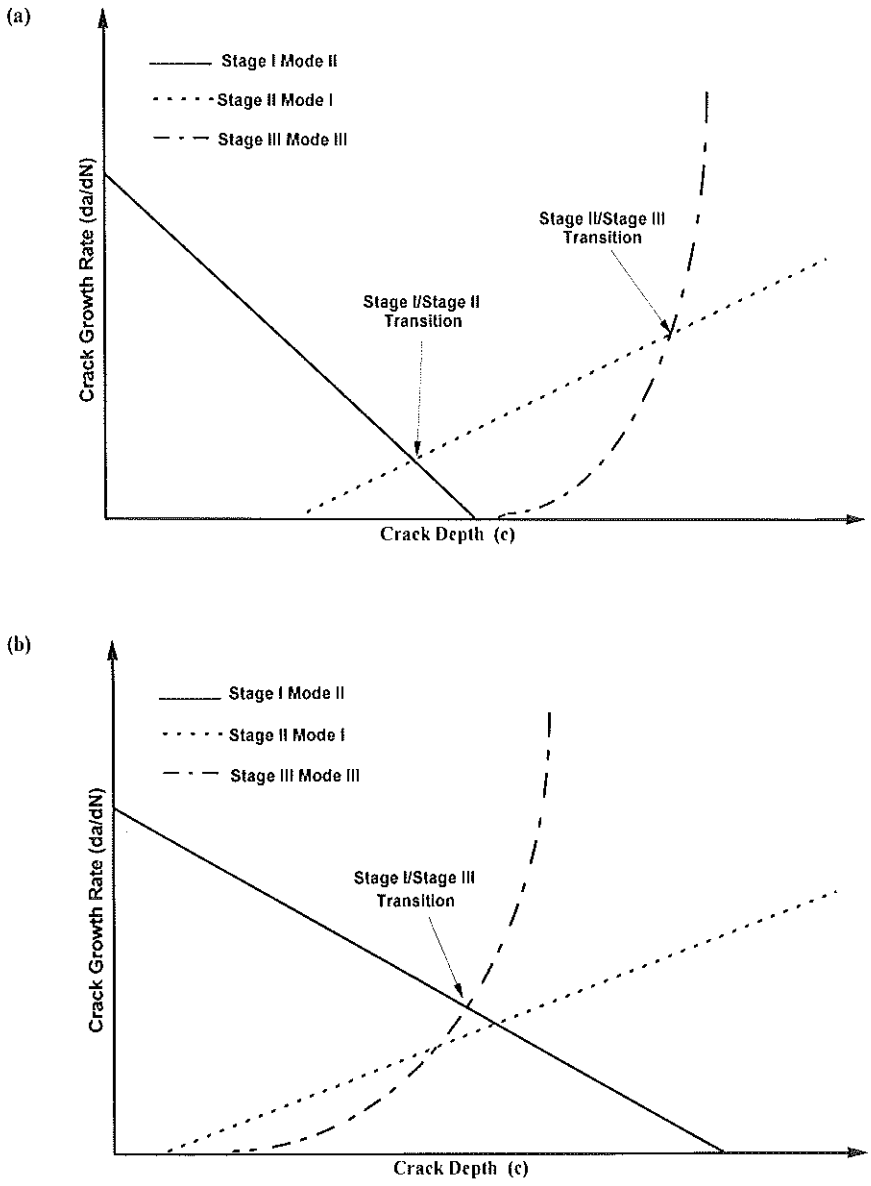

Fig 9 Torsional crack path criterion for (a) high-cycle fatigue, and (b) low-cycle fatigue.

5 A General Approach to Fatigue Life Prediction

Rules for FCG under three modes of loading for medium carbon steel have been obtained, which assist the development of a model to estimate the number of cycles to grow a crack to a critical size, and to predict crack path. A crack will extend in the mode which enables the easiest or fastest propagation rate (**8**). An experimental programme has been conducted on solid cylindrical specimens of 0.4C steel with a uniform gauge length of 30 mm (10 mm diameter) subjected to reversing torsion at room temperature. In high-cycle fatigue (HCF) cracks start propagation in Stage I, then tend to deviate to become more nearly perpendicular to the maximum principal stress (Fig. 5b). In LCF cracks propagate in Stage I for a few cycles, showing a minimal degree of Stage II and quickly becoming Stage III shear cracks, which is the dominant mode in this region, as shown in Fig. 9. Although this study concentrated on torsional behaviour, the methodology is equally applicable to tension–compression (**2**), and any other mode of loading. Thus a framework is provided for a general fatigue life prediction procedure.

5.1 *Predicting crack path for each stage*

The transition from one stage to another is estimated by assuming that a fatigue crack will adopt the fastest mode for propagation (**8**), so that in Fig. 9, for each crack length the highest FCG curve from the three candidate mechanisms operates. At the critical crack length for transition

$$[\mathrm{d}c/\mathrm{d}N]_x = [\mathrm{d}c/\mathrm{d}N]_y \tag{13}$$

For the transition from Stage II (Mode I) to Stage III (Mode III), taking $x = \mathrm{I}$ and $y = \mathrm{III}$ gives a critical length c_d from equations (6) and (10), see Fig. 9a. At rather higher strain levels, there is sufficient plasticity to sustain Mode III crack growth, so that propagation in Mode III can be achieved without passing through a phase of Mode I. This crack length can be estimated with $x = \mathrm{II}$ and $y = \mathrm{III}$ from equations (2) and (10), see (Fig. 9b). More usually, the classical Stage I to Stage II transition occurs ($x = \mathrm{II}$ and $y = \mathrm{I}$ with equations (2) and (6) yielding c_i).

5.2 *Life prediction method*

To predict fatigue lifetime theoretically two sources of crack propagation data have been used, taken from Hobson (**2**) and Fig. 6. Hobson's work concerned Stage I and II fatigue crack propagation, and was employed to determine the fatigue life for those stages, by using equations (3) and (7). Because of the paucity of Mode III data for flat fracture on a transverse plane in torsion, new crack growth rate results were generated.

A global prediction for the fatigue life has been derived, which is compared to the experimental results for torsional fatigue endurance. Both theoretical and

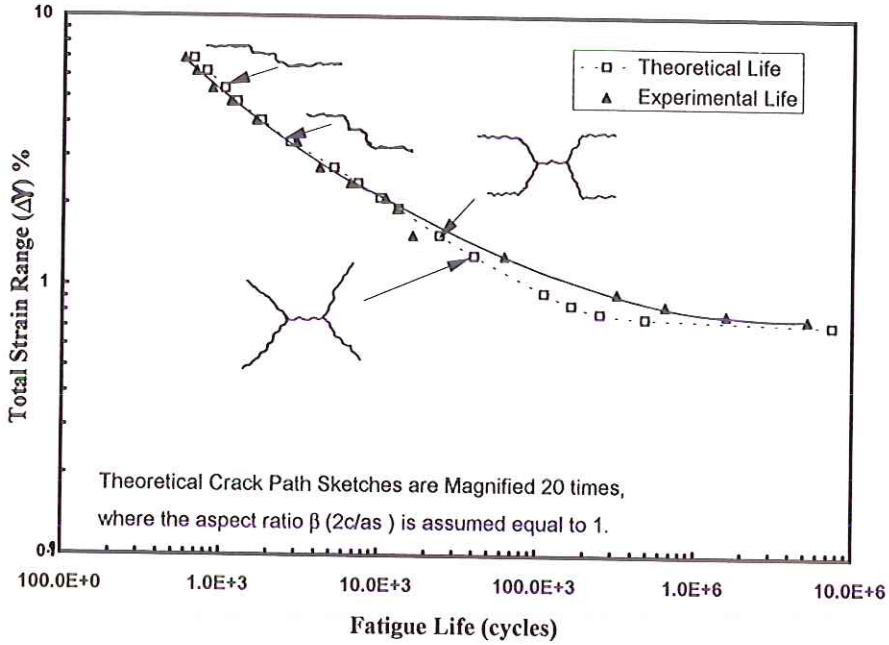

Fig 10 Theoretical and experimental torsional strain life curves for medium carbon steel.

experimental fatigue lifetimes versus shear strain range are plotted together in Fig. 10, which gives a clear indication of how the predicted results compare. The estimation of life shows less than 35% error compared to the experimental endurance in the high strain region. A more significant difference appears in the transition stage from high strain fatigue down to the fatigue limit, where life predictions are conservative, probably because no attempt was made to allow for crack closure or fracture surface roughness effects on propagation.

5.3 *Failure mode prediction*

Predicting the crack depth for each mode of propagation depends on the criterion that fatigue cracks grow in the shear modes, if there is sufficient plasticity to support them, otherwise cracks turn to grow in the tensile stress mode. Crack path was predicted from the FCG laws for three stages, equations (2, 6, 10). In experiment, Stage I was observed on the maximum shear plane up to the transition depth with Stage II in HCF on 45° planes as expected, whereas for LCF shear mode FCG occurred up to failure (Fig. 10). Predictions were less good in the middle region between HCF and LCF, because no account was taken for the effects of crack face friction in equation (13).

6 Conclusions

Some general conclusions on multiaxial fatigue crack propagation can be drawn from this overview.

(1) Four mechanisms of fatigue crack growth can be observed in practice for ductile metals, three of which involve crack extension on planes of maximum shear stress and strain.
(2) Crack propagation rates for each mechanism may be characterized by LEFM/EPFM laws.
(3) Thresholds for propagation exist for each mode except Stage I, which enables cracks to initiate rapidly from machined or polished surfaces.
(4) Fatigue life prediction and crack path to failure may be predicted by integration of the four propagation laws, using a maximum growth rate criterion for selection of the current crack extension mechanism.

Acknowledgements

The authors are thankful to the numerous research staff in SIRIUS who, over many years, have conducted fatigue tests and generated the concepts reviewed in this paper. We are also indebted to the many industries and government organizations who have sponsored the research.

References

(1) BROWN, M. W. (1986) Interfaces between short, long and nonpropagating cracks, *The Behaviour of Short Fatigue Cracks*, European Group on Fracture Publication No. 1 (editors K. J. Miller and E. R. de los Rios), Mechanical Engineering Publications Limited, London, pp. 423–439.
(2) HOBSON, P. D. (1985) The growth of short fatigue cracks in a medium carbon steel, Ph.D. thesis, The University of Sheffield, U.K.
(3) PEREZ CARBONELL, E. and BROWN, M. W. (1986) A study of short crack growth in torsional low cycle fatigue for a medium carbon steel, *Fatigue Fract. Engng. Mater. Struct.*, **9**, pp. 15–33.
(4) LEBLOND, J. B. (1993) Crack kinking and curving in three-dimensional elastic solids, *Mixed-mode Fatigue and Fracture*, ESIS Publication No. 14 (editors H. P. Rossmanith and K. J. Miller), Mechanical Engineering Publications, London, pp. 219–243.
(5) BROWN, M. W. and BUCKTHORPE, D. E. (1989) A crack propagation based effective strain criterion, *Biaxial and Multiaxial Fatigue*, European Group on Fracture Publication No. 3 (editors M.W. Brown and K.J. Miller), Mechanical Engineering Publications, London, pp. 499–510.
(6) BROWN, M. W. (1988) Aspects of fatigue crack growth, *Proc. I. Mech. Engrs*, **202**, (C1), 19–29.
(7) BROWN, M. W. and MILLER, K. J. (1973) A theory for fatigue failure under multiaxial stress strain conditions, *Proc. I. Mech Engrs*, **187**, pp. 745–755.
(8) HOURLIER, F., d'HONDT, H., TRUCHON, M. and PINEAU, A. (1985) Fatigue crack path behaviour under polymodal fatigue, *Multiaxial Fatigue*, ASTM Special Technical Publication 853 (editors K. J. Miller and M. W. Brown), American Society for Testing and Materials, Philadelphia, pp. 228–248.
(9) SOMMER, E. (1969) Formation of fracture lances in glass, *Engng Fract. Mech.*, **1**, pp. 539–546.
(10) RITCHIE, R. O., McCLINTOCK, F. A., TSCHEGG, E. K. and NAYEB-HASHEMI, H. (1985) Mode III fatigue crack growth under combined torsion and axial loading, *Multiaxial Fatigue*, ASTM Special Technical Publication 853 (editors K. J. Miller and M. W. Brown), American Society for Testing and Materials, Philadelphia, pp. 203–227.

(11) POOK, L. P. (1985) The fatigue crack direction and threshold behaviour of mild steel under mixed Mode I and III loading. Int. J. Fatigue **7**, pp. 21–30.
(12) HAY, E. and BROWN, M. W. (1986) Initiation and early crack growth of fatigue cracks from a circumferential notch loaded in torsion, *The Behaviour of Short Fatigue Cracks*, European Group on Fracture Publication No. 1 (editors K. J. Miller and E. R. de los Rios), Mechanical Engineering Publications Limited, London, pp. 309–321.
(13) TSCHEGG, E. K., RITCHIE, R. O. and McCLINTOCK, F. A. (1983) On the influence of rubbing fracture surfaces on fatigue crack propagation in Mode III, *Int. J. Fatigue*. **5**, pp. 29–35.
(14) TSCHEGG, E. K. (1983) Mode III and Mode I fatigue crack propagation behaviour under torsional loading, *J. Mater. Sci.*, **18**, pp. 1604–1614.
(15) YATES, J. R. (1987) Crack tip plastic zone sizes in cylindrical bars subjected to torsion, *Fatigue Fract. Engng. Mater. Struct.*, **10**, pp. 471–477.
(16) POOK, L. P. and SHARPLES, J. K. (1979) The Mode III fatigue crack growth thresholds for mild steel, *Int. J. Fracture*, **15**, pp. R223–R225.
(17) POOK, L. P. and GREENAN, A. F. (1979) Fatigue crack growth threshold in mild steel under combined loading, *Fracture Mechanics*, ASTM Special Technical Publication 677, American Society for Testing and Materials, Philadelphia, pp. 23–35.
(18) TSCHEGG, E. K. (1982) A contribution of Mode III fatigue crack propagation, *Mater. Sci. Engng.*, **54**, pp. 127–136.
(19) YATES, J. R. and MILLER, K. J. (1989) Mixed Mode (I + III) fatigue thresholds in a forging steel, *Fatigue Fract. Engng. Mater. Struct.* **12**, pp. 259–270.
(20) POOK, L. P. (1980) Mode I branch cracks and their implication for combined mode failure. NEL Report No 667, Department of Industry, April 1980.
(21) McCLINTOCK, F. A. and TSCHEGG, E. K. (1984) On the plastic zone size in circumferentially grooved shafts at high torques, *Int. J. Fract.*, **26**, pp. R11–R14.
(22) HURD, N. J. and IRVING, P. E. (1982) Factors influencing propagation of Mode III fatigue cracks under torsional loadings, *Design of Fatigue and Fracture Resistant Structures*, ASTM Special Technical Publication 761, American Society for Testing and Materials, Philadelphia, pp. 212–233.
(23) YOSHIOKA, S., WATANABE, K., KITAGAWA, H., INOUE, A. and KUMASAWA, M. (1984) Fatigue crack growth threshold (ΔK_{th}) under Mode III (the effect of stress ratio and mixed mode), *Fatigue 84*, (editor C.J. Beevers), Engineering Materials Advisory Services, Warley, U.K., pp. 241–253.
(24) YATES, J. R. and MOHAMMED, R. A. (1993) The effect of mean stress on mixed Mode (I + III) fatigue thresholds, *Fatigue Fract. Engng Mater. Struct.*, **16**, pp. 1355–1363.
(25) TONG, J., YATES, J. R. and BROWN, M. W. (1994) The influence of precracking techniques on fatigue crack growth thresholds under mixed mode I/II loading conditions, *Fatigue Fract. Engng. Mater. Struct.*, **17**, pp. 1261–1269.
(26) ROSSMANITH, H. P. and MILLER, K. J. (editors) (1993) *Mixed-mode Fatigue and Fracture*, ESIS Publication No. 14, Mechanical Engineering Publications, London.
(27) BOLD, P. E., BROWN, M. W. and ALLEN, R. J. (1991) Shear mode crack growth and rolling contact fatigue, *Wear*, **144**, pp. 307–317.
(28) WONG, S. L., BOLD, P. E., BROWN, M. W. and ALLEN, R. J. (1996) A branch criterion for shallow angled rolling contact fatigue cracks in rails, *Wear*, **191**, 45–53.